Supplementary Information

Non-noble metal loaded schiff-base based covalent organic polymers as efficient electrocatalysts for OER

Xinming Hu[#], Xiao Yang[#], Zitong He, Xun Tian, Penglei Cui*, Tao Meng*, Xiang Cheng

College of Science,Hebei Agricultural University, Baoding 071001, PR China

This PDF file includes:

Table of contents:

Chemicals such as vanillin, trichlorotriazine, 2,6-diaminoanthraquinone, triethylamine (TEA), 1,4-dioxane, methanol, anhydrous ethanol, ethyl acetate, $Fe(NO_3)_3$, $Ni(NO_3)_2$, $Co(NO_3)_2$, N,N-Dimethylformamide (DMF), Nickel foam (NF), and Nafion (5 wt%) were sourced from Energy Chemical Co., Ltd. All chemicals employed were of analytical standard and directly used without further purification. The crystallographic analysis of the samples was performed via X-ray powder diffraction (XRD) using a Bruker D8 Advance instrument equipped with Cu Kα radiation (λ=1.5406 Å) over a 2θ range of 10° to 80°. Morphological and elemental analysis were conducted using scanning electron microscopy (SEM) coupled with energy dispersive X-ray spectroscopy (EDS) on a ZEISS sigma500 instrument. Additional characterization was achieved through transmission electron microscopy (TEM) on a JEOL-JEM 2100F system. The surface area and porosity of the samples were evaluated by nitrogen adsorption-desorption isotherms and Brunauer-Emmett-Teller (BET) analysis on a BELSORP MaxII analyzer. Fourier transform infrared (FT-IR) spectroscopy (BeiRei-Ruili WQF-510) was utilized for structural identification. The surface chemistry was explored by X-ray photoelectron spectroscopy (XPS) on a ThermoFisher Nexsa platform. Lastly, nuclear magnetic resonance (NMR) spectra for ^1H were recorded on a Bruker 400M spectrometer.

In a typical procedure, vanillin (0.01 mol) and triethylamine (0.012 mol) were dissolved in 12 mL 1,4-dioxane, and the resulting solution was stirred for 10 minutes. Subsequently, a solution of cyanuric chloride (0.0025 mol) in 6 mL 1,4-dioxane was carefully added dropwise to the mixture. The reaction was maintained at ambient temperature for approximately 10 hours. After this period, the temperature was increased to 85°C, and the reaction was continued for an additional 8 hours. Upon completion, the reaction mixture was cooled to room temperature. The precipitate formed was isolated by filtration and washed with ethanol. Further purification was achieved by recrystallization of the solid from ethyl acetate, yielding a white crystalline product, which was identified as TMPT-CHO.

In a 100 mL round-bottom flask, 0.4 mmol TMPT-CHO and 0.6 mmol 2,6-diaminoanthraquinone were added. The mixture was then degassed and purged with nitrogen to ensure an inert atmosphere. Subsequently, 15 mL DMF was added to the flask, and the resulting solution was refluxed under nitrogen for about 14 hours. Upon completion, the mixture was cooled to room temperature, resulting in the formation of a yellow precipitate. The solid product was isolated by vacuum filtration and further purified by Soxhlet extraction with methanol for approximately two days. Finally, the extracted solid was dried overnight under vacuum at 60°C to yield the desired covalent organic polymer (COP).

100 mg as-prepared COP was processed into a fine powder and uniformly dispersed in 20 mL distilled water, followed by ultrasonic treatment for 15 minutes. Subsequently, 30 mg $Fe(NO_3)_3$, $Co(NO_3)_2$, and $Ni(NO_3)_2$ were separately dissolved in 2 mL distilled H_2O, and these salt solutions were individually introduced into the aforementioned COP solution. The mixture was then subjected to reaction under refluxing for approximately 4 hours. The resulting solid, obtained by completely evaporating the solvent in vacuum, was washed several times with distilled H_2O to yield M-COP (Fe-COP, Co-COP, and Ni-COP) (Scheme 1).

Firstly, 4 mg the powdered catalyst (M-COP) and 2 mg carbon powder were placed in a 1.5 mL centrifuge tube. Subsequently, absolute ethanol (950 μL) and 0.5 wt% Nafion solution (20 μL) were introduced into the tube. The combined solution was then vigorously agitated through ultrasonic treatment for a duration of 50 minutes to ensure homogeneous dispersion. Afterward, 80 μL this uniformly mixed solution was precisely dispensed and uniformly applied onto the surface of a NF conductive substrate, with a specified coating area of 1 cm × 0.7 cm. The coated substrate was allowed to dry at room temperature for subsequent use.

Electrochemical assessments were performed utilizing a standard three-electrode configuration facilitated by a CHI760E electrochemical workstation sourced from Shanghai Chenhua Instruments Co. Ltd. The specimens, mounted onto nickel foam substrates, were directly integrated as the operative electrode with a defined geometric surface area of 0.7 cm^2. For the purpose of reference and counter electrodes, Ag/AgCl and a graphite rod were respectively employed.

OER examinations were carried out in an O_2-saturated 1.0 M KOH electrolyte (pH = 14.0). The polarization curve data underwent identical iR compensation at 90% and were then translated into potentials versus the reversible hydrogen electrode (RHE), leveraging the Nernst equation: E(RHE) = E(Ag/AgCl) + 0.197 V + 0.059 V/pH unit × pH. The overpotential (η) for OER was derived using the equation: η = E(RHE)-1.23 V, where 1.23 V corresponds to the equilibrium potential of the H_2O/OH^- redox couple in alkaline media. Additionally, stability evaluations were performed at a fixed current density of 10 mA cm^{-2}. The ECSA was measured through the double-layer capacitance (Cdl) by acquiring CV curves at different scan rates (20, 40, 60, 80, 100 mV s^{-1}) within a non-Faradaic potential window of 0.02 to 0.12 V vs. Ag/AgCl. EIS was recorded at an overpotential of 300 mV, spanning a frequency range of 0.01 to 100 kHz. The stability of the catalyst electrode was evaluated using chronopotentiometry at a current density of 10 mA cm^{-2} for 24 hours.

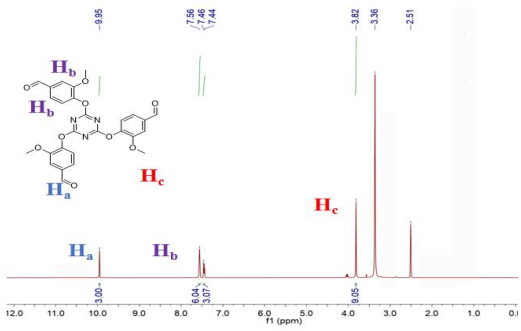

Fig. S1 ^{1}H NMR of TMPT-CHO

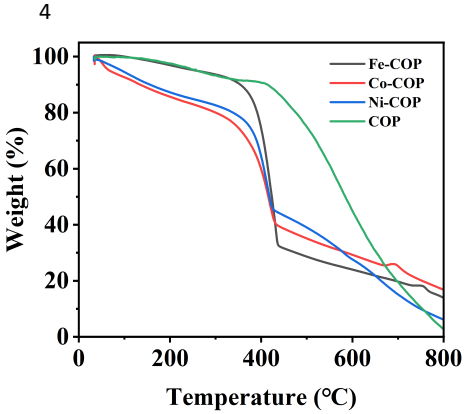

Fig. S2 TGA of M-COP

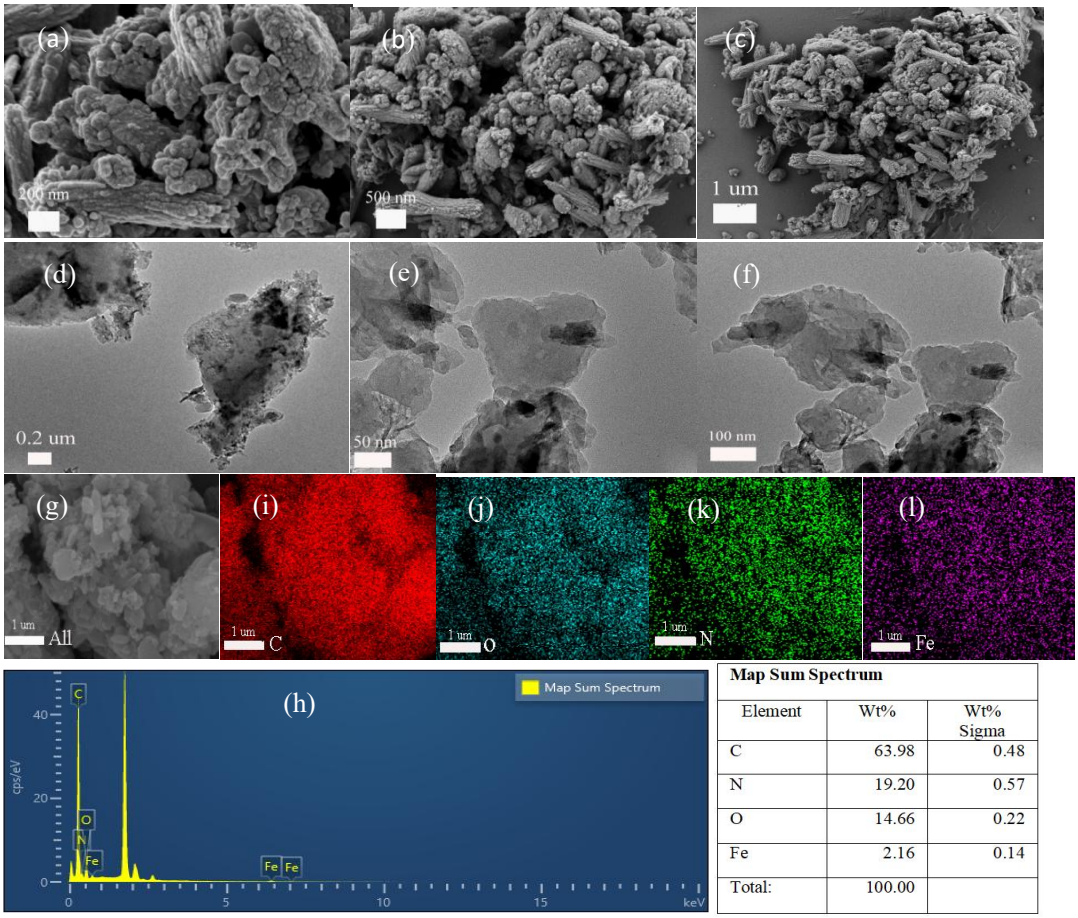

Map Sum Spectrum		
Element	Wt%	Wt% Sigma
C	63.98	0.48
N	19.20	0.57
O	14.66	0.22
Fe	2.16	0.14
Total:	100.00	

Fig. S3a SEM images (a-c) and TEM (d-f) of Fe-COP at different magnifications; SEM-EDS element content graph mapping (g) of Co-COP; EDS elemental mappings of C (i), O (j), N(k), Co (l), in the Co-COP electrocatalyst (h)

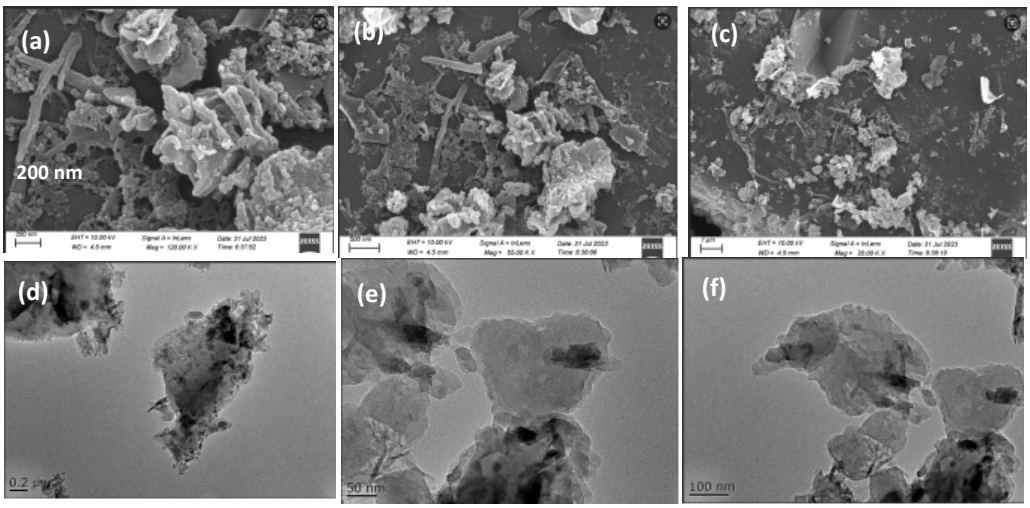

Fig. S3b SEM images (a-c) and TEM (d-f) of Ni-COP at different magnifications

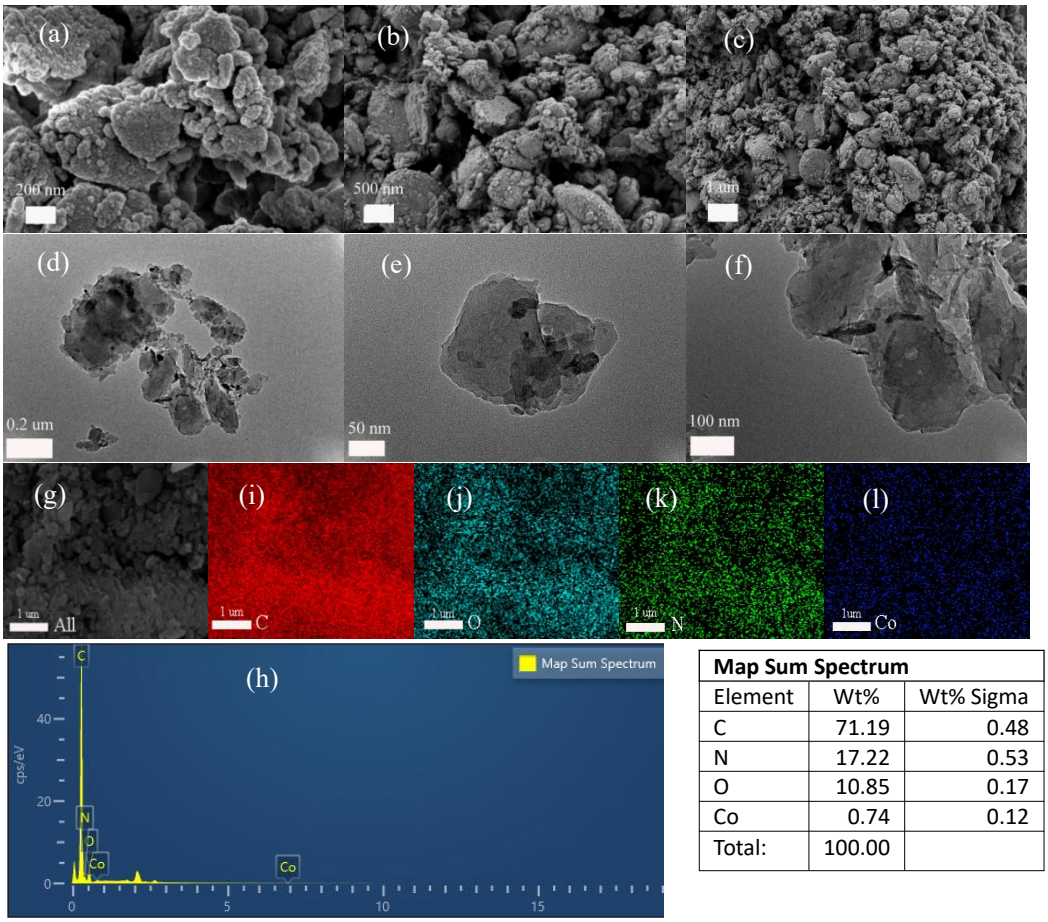

Map Sum Spectrum		
Element	Wt%	Wt% Sigma
C	71.19	0.48
N	17.22	0.53
O	10.85	0.17
Co	0.74	0.12
Total:	100.00	

Fig. S4 SEM images (a-c) and TEM (d-f) of Co-COP at different magnifications; SEM-EDS element content graph mapping (g) of Co-COP; EDS elemental mappings of C (i), O (j), N(k), Co (l), in the Co-COP electrocatalyst (h)

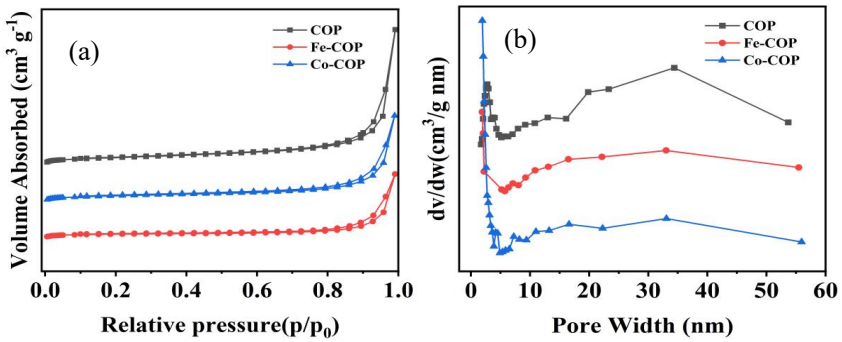

Fig. S5 Nitrogen adsorption and desorption curve (a) and pore size distribution (b) of COP, Fe-COP, and Co-COP

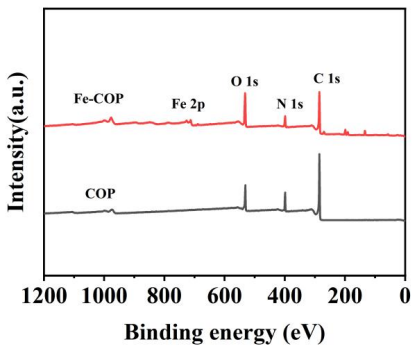

Fig. S6a XPS survey scan of COP and Fe-COP

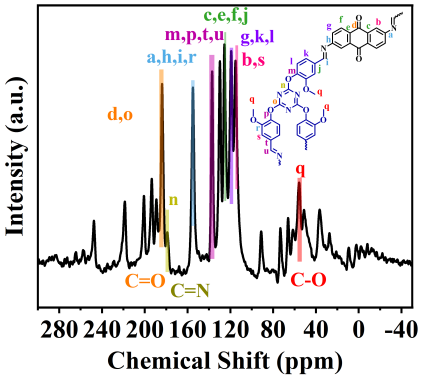

Fig. S6b ^{13}C CP/MAS NMR of COP

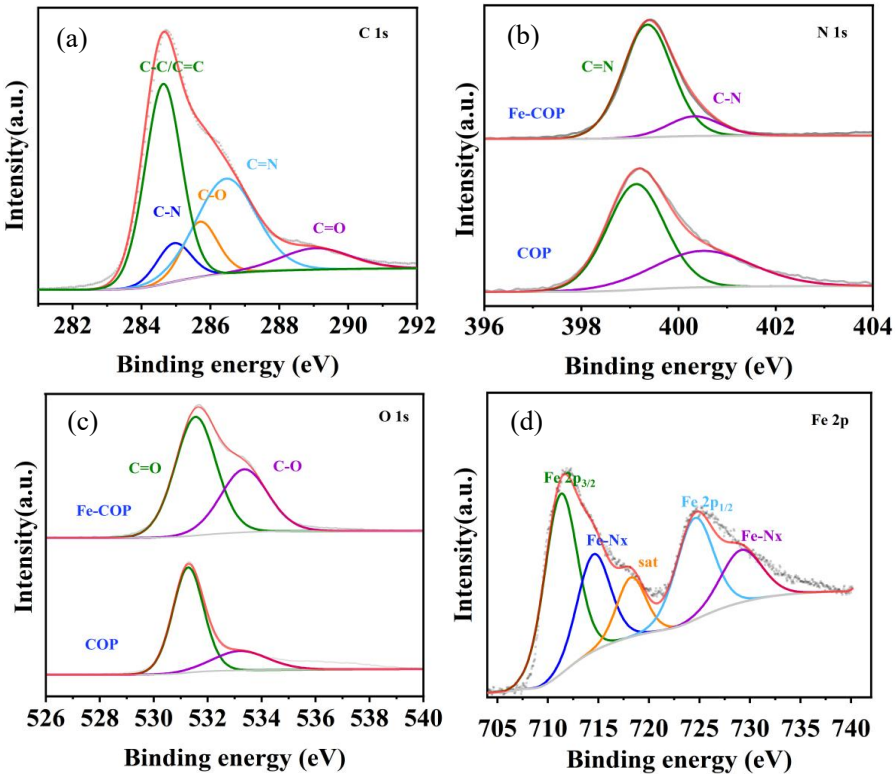

Fig. S7. XPS deconvoluted spectra of Fe-COP for C 1s (a), N 1s (b), O 1s (c), Fe 2p (d).

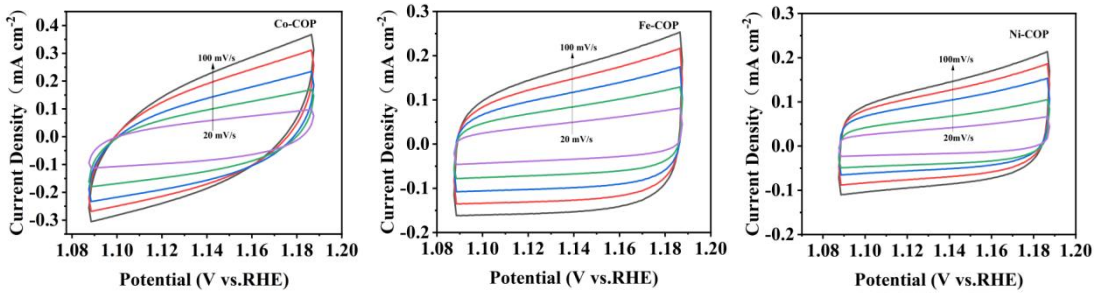

Fig. S8 Cyclic voltammetry (CV) of Co-COP(a), Fe-COP(b) and Ni-COP(c) at different scan rates in OER.

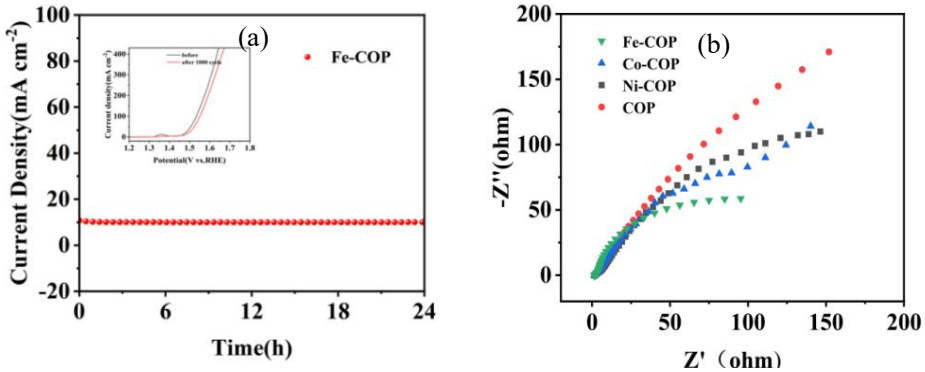

Fig. S9 (a) chronoamperometry of Fe-CoP at 1.53 V over 24 h (inset: LSV before and after OER reaction) (b) Nyquist plots obtained by EIS at 1.53V *vs*. RHE

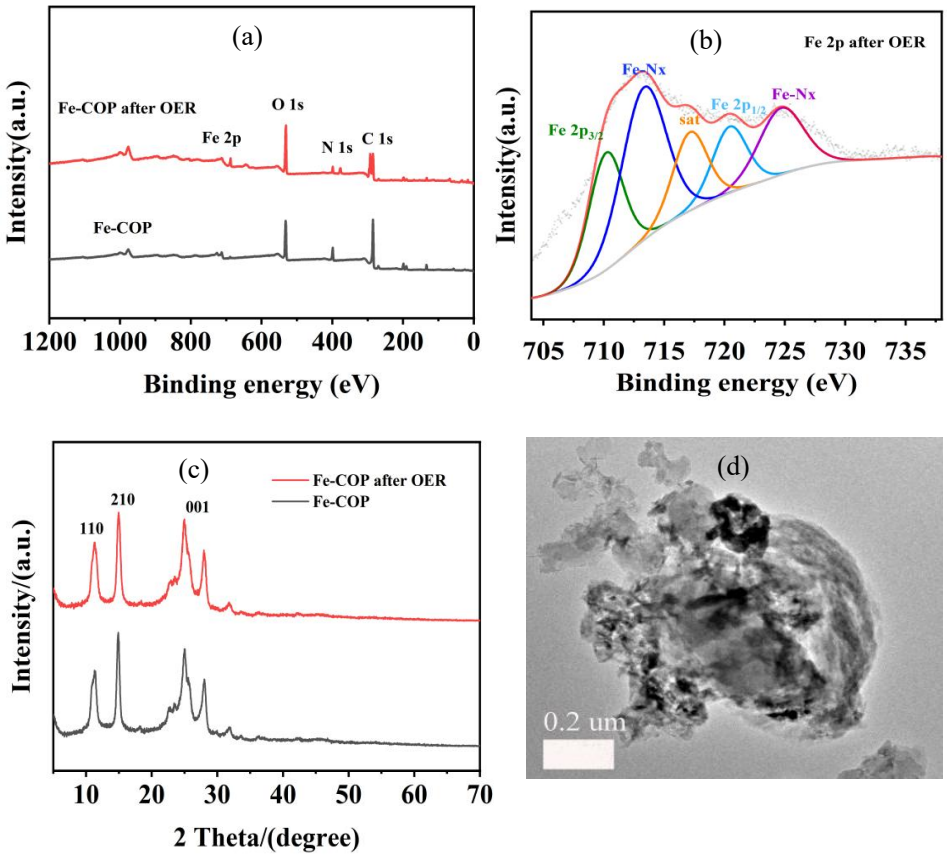

Fig. S10 XPS survey scan of Fe-COP before and after OER (a); Fe 2p after OER (b); XRD of Fe-COP before and after OER (c); (d) TEM of Fe-COP after OER.

Table S1. The comparison of the electrocatalytic OER of different catalytic systems

Sample	Application	Electrolyte	Current Density (mA/cm^{-2})	Overpotential (mV)	Tafel slope ($mV\ dec^{-1}$)	Ref.
Ni-COF	OER	1M KOH	10	302	56	[1]
COF-TpDb-TZ-Co	OER	1M KOH	10	400	82	[2]
Co@COF-Pyr	OER	1M KOH	10	400	100	[3]
NiPc–Ni	OER	1M KOH	10	319	83	[4]
macro-TpBpy-Co	OER	0.1M KOH	10	380	89	[5]
Ni-COF	OER	0.1M KOH	10	302	56	[6]
Co-MCOF	OER	0.1M KOH	10	268	80	[7]
FX-FeCo-TPP	OER	1M KOH	10	251	35.2	[8]
Fe-COP	OER	1M KOH	10	233	54.6	This work

References

1 M. Punniyamoorthy, S. S. Roy, M Kathiresan and S Kundu, *Acs. Appl. Energ. Mater.,* 2024, 7 4111.

2 Y. Liang, T. Xia , Z. Wu, Y. Yang, Y. Li, Z. Sui, C. Li, R. Fan, X. Tian and Q. Chen, *Mater. Today Chem.,* 2022, **24**, 100777.

3 Y. Zhao, Y. Yang, T. Xia, H. Tian, Y. Li, Z. Sui, N. Yuan, X. Tian and Q. Chen, *ChemSusChem* 2021,*14*, 4556.

4 J. W. Li, P. Liu, J. X. Mao, J. Y. Yan and W. B. Song, *J. Mater. Chem. A*, 2019, **21**, 1279.

5 X. J. Zhao, P. Pachfule, S. Li, T. Langenhahn, C. Schlesiger, S. Praetz, J. Schmidt and A. Thomas, *J. Am. Chem. Soc*., 2019,**16**, 6623.

6 M. Punniyamoorthy, S. Singha Roy, M. Kathiresan and S. Kundu, *ACS Appl. Ener. Mater.*, 2024, **7 (9)**, 4111.

7 C. Lin, H. Ma, J. He, Q. Xu, M. Song, C. Cui, Y. Chen, C. Li, M. Jiao and L. Zhai, *Small,* 2024, **20**, 2403775.

8 X. M. Hu, P. L. Cui, H. Zhang and Z. T. He, *New J. Chem*., 2024, **48 (22)**, 10126.